Surface Science Letters

Analysis of carbon nanotube pull-out from a polymer matrix

S.J.V. Frankland, V.M. Harik *

ICASE, MS 132C, NASA Langley Research Center, Hampton, VA 23681-2199, USA

Abstract

Molecular dynamics simulations of carbon nanotube (NT) pull-out from a polymer matrix are carried out. As the NT pull-out develops, variations in the displacement and velocities of the NT are monitored. The existence of a carbon-ring-based period in NT sliding during pull-out is identified. Linear trends in the NT velocity–force relation are observed and used to estimate an effective viscosity coefficient for interfacial sliding at the NT/polymer interface. As a result, the entire process of NT pull-out is characterized by an interfacial friction model that is based on a critical pull-out force, and an analog of Newton's friction law used to describe the NT/polymer interfacial sliding.
© 2002 Elsevier Science B.V. All rights reserved.

1. Introduction

Polymer nanocomposites with carbon nanotubes (NTs) have been fabricated and mechanically tested to explore their potential as strong, lightweight materials [1–3]. While some reinforcement of the polymer has been observed in the form of enhanced stiffness, a detailed understanding of the NT/polymer interface remains fundamental to the optimization of their properties. The interface plays a significant role in the stress transfer and the consequent improvements in stiffness and strength. Characterization of the NT/polymer interfacial interactions during NT sliding is the focus of this study.

For traditional fiber-reinforced polymer matrix composites, the interfacial shear strength is typically evaluated by fiber pull-out [4] or fiber push-out tests [5]. The fiber decohesion process is characterized by the *critical shear stress* required to debond the fiber. This shear stress value is estimated from the critical axial load using the shear-lag model. For nanocomposites, a similar procedure can be utilized both experimentally [6] and theoretically [7]. For a NT embedded in a polymer, the critical shear stress has been evaluated via molecular dynamics (MD) simulations and the shear-lag model [7]. This study extends the previous work to develop analysis of NT/polymer interfacial sliding.

At the nanoscale, interfacial sliding is closely linked with the fundamental origins of sliding friction. Friction seems to originate mainly from

_____
* Corresponding author. Current address: Swales Aerospace, MS 186A, NASA LaRC, Hampton, VA 23681, USA. Tel.: +1-757-864-2195; fax: +1-757-864-9668.

E-mail addresses: s.j.frankland@larc.nasa.gov (S.J.V. Frankland), v.m.harik@larc.nasa.gov (V.M. Harik).

the sliding induced excitation of atomic lattice vibrations and electronic motion [8,9]. These friction mechanisms have been studied by a quartz-crystal microbalance [10,11], scanning force microscopy [12,13] and complementary theoretical modeling [8].

In the system simulated here, the matrix is crystalline polyethylene (PE), which interacts with the NT via van der Waals forces represented by the Lennard-Jones potential. NT velocity and displacements are traced in order to characterize the interfacial interactions during NT pull-out. The NT/polymer interfacial friction is described with a relation between the applied force and NT velocity. Furthermore, an interfacial friction model for the entire pull-out process is proposed, which involves an effective viscosity coefficient for the interfacial sliding.

2. Molecular structure of the nanotube/polymer system

The nanoscale material system in this study is composed of a carbon NT and a PE matrix. Specifically, a (10,10) carbon NT is embedded in crystalline polymer matrix (Fig. 1(a) and (b)). The system contains about 23,000 atoms including an 880-C-atom NT and 178 chains of 42 methylene units with the hydrogen atoms explicitly included. The dimensions of the system are $\sim 6 \times 6 \times 6$ nm. In the MD simulations, the entire system is rep-

resented with the hydrocarbon potential developed by Brenner et al. [14]. The system is replicated across periodic boundaries in each of the three-dimensions, thereby making the NT and the PE chains infinitely long. This composite is similar to the crystalline non-bonded PE one used in the previous work [7], and the detailed chemical description is kept for consistency.

The entire NT pull-out process is simulated by MD. As the sample cell is periodic, the pull-out is simulated by pulling the NT through, rather than out of the PE matrix. A unidirectional force is applied to each atom of the NT along the NT axis. The applied force is increased incrementally over time (Fig. 2). The simulation is run for $\sim 100,000$ MD time steps of 0.5 fs. Data generated from the MD simulation of this system forms the input to the interfacial friction model described below.

3. Simulation and characterization of nanotube pull-out

The MD simulation captures the entire NT pull-out process. Initially, sliding begins after a sufficient amount of force is applied to the NT. In Fig. 2, the increments of applied force are shown, and over time, the velocity (Fig. 2) and the displacement (Fig. 3) of the NT are monitored. In the simulation, the axial velocity of the NT is sufficiently greater than the velocity of the surrounding polymer, and the latter is therefore neglected in the
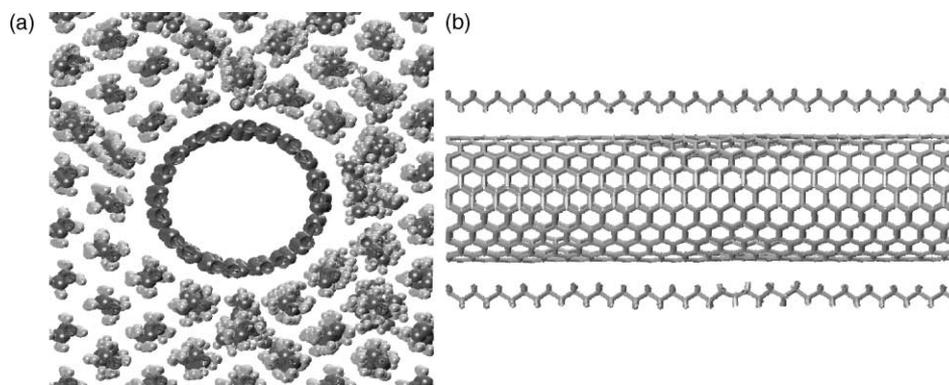

Fig. 1. Molecular structure of crystalline PE/NT composite: (a) a cross-section of the central 3.6 nm region of the sample and (b) a side view of the NT and two nearby PE chains.
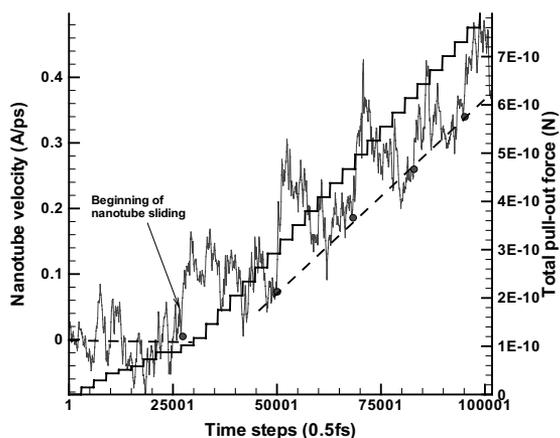
Fig. 2. Velocity of the center of mass of a carbon NT during the simulated pull-out and the increments of axial force applied to the NT over time.
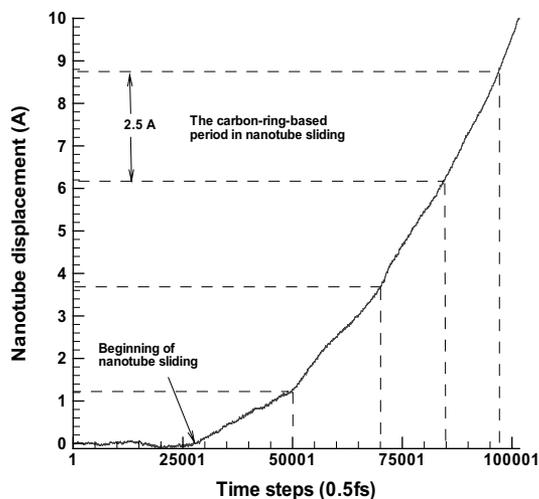

Fig. 3. Displacement of individual carbon atoms of the NT during the pull-out process.

analysis. A detailed analysis of the NT velocity data is subsequently carried out to characterize the pull-out process, in general, and interfacial sliding, in particular. [1]

Following the observed variations in the axial velocity of the NT, the entire pull-out process can be divided into several stages. Prior to the onset of sliding, the NT experiences thermal vibrations and interacts with the adjacent polymer chains in equilibrium at 300 K for the first 27,000 time steps (up to the time of pull-out, $t_{\text{pull-out}}$) as the applied force is being gradually increased to 0.1 nN. Beyond this critical force, the NT starts to slide through the polymer. Following the details of the MD simulation results presented in Figs. 2 and 3 as well as the established conceptual framework for viscoplastic interfacial yielding [15], the entire NT pull-out process can be described by four stages.

(1) Initially, equilibrium exists between the NT and the surrounding polymer ($t < t_{\text{pull-out}}$).
(2) At an applied force of about 0.1 nN, an accession of the energy/force barrier occurs initiating slippage between the NT and the polymer. This onset of slippage is marked by a noticeable increase in the axial velocity of the NT, which is observed at $t = t_{\text{pull-out}}$.
(3) Slippage of the NT in the polymer cavity fully develops during a transition stage between $t_{\text{pull-out}}$ and $t_{\text{ss}} \approx 50{,}000$ time steps, where t_{ss} refers to the onset of steady sliding.
(4) The steady sliding of the NT ($t > t_{\text{ss}}$) is characterized by semi-periodic variations in the NT sliding velocity as the NT accelerates under step-wise increases in the applied force. The onset of periodic accelerations in the NT sliding is marked by dots in Fig. 2.

Similar stages of interfacial sliding have been observed for other surfaces [9].

The observed periodic variations in the NT axial velocity (Fig. 2) can be related to the size of the carbon rings in the NT periodic structure (Fig. 1b). From a comparison of the velocity and displacement data in Figs. 2 and 3, a correlation is evident between the NT displacement and the period of the velocity oscillations. The NT movement can, therefore, be scaled by the width of a carbon ring, a. In Fig. 2, the dots on the velocity trace mark the onset of accelerations, which are related to the ascent of local energy barriers at the beginning of the carbon ring period. In the displacement trace plotted in Fig. 3, the changes in

the slope, marked by the dotted lines, occur simultaneously with the beginning of the accelerations in the NT velocity in Fig. 2. These changes in the slope are separated by 2.46 A, the width of the carbon rings, a. Such spatially quantized friction with an atomic lattice periodicity has been also observed for other systems [13].

4. Nanoscale friction laws and an interface model

For fiber-reinforced composites, interfacial debonding and sliding can be simulated by viscoplastic models for matrices accompanied by an interface potential [15]. A Bingham-type model [15] for viscoplastic failure of the interface relates the shear stress, τ, to the strain rate, $\dot{\gamma}$, by Newton's constitutive law ($\tau = \mu\dot{\gamma}$) [16] after the yield stress, τ_0, is reached:

$$\tau = \tau_0 + \mu_m\dot{\gamma}. \tag{1}$$

Here, μ and μ_m are viscosities of a fluid and a viscous matrix material, respectively. Newton's constitutive law [16] is defined for the adjacent layers of a continuum fluid that is subjected to shearing. Experimentally, such interfacial viscosities of monolayers on surfaces can be deduced from measurements with a quartz-crystal microbalance [10]. At the nanometer level, an analog of Newton's law can be applied, which relates the force applied and NT velocity (Fig. 4) to determine an effective viscosity of interfacial sliding. The stresses and strain rates can be recast in terms of average forces and velocity gradients derived from the MD simulations.

In order to model the sliding between a NT and the surrounding polymer chains on a lengthscale level larger than the carbon rings, multiple carbon ring lengths of simulation data are needed for sufficiently meaningful averaging of contributions from the local NT structure. The relative sliding involves two surfaces, that is, the NT and polymer. In the longitudinal direction, the NT length, L_{NT}, should be sufficiently long, that is, $L_{NT}/a > 10$, where a is the width of a carbon ring. The number 10 implies an order of magnitude difference. Likewise, for the perimeter of the NT/polymer interface, the NT radius should satisfy a similar
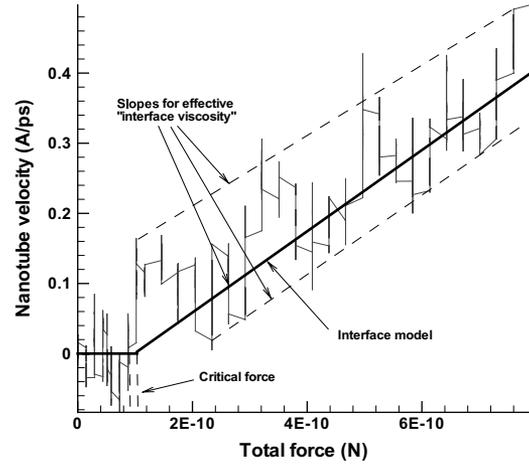

Fig. 4. Comparison between the interface friction model and the MD simulation data.

inequality: $2\pi(R_{NT} + \bar{h}_{VdW}/2)/a > 10$, where R_{NT} is the NT radius and $\bar{h}_{VdW}$ is an average surface separation caused by the van der Waals forces. The considered NT/polymer system satisfies all these averaging (or homogenization [17]) criteria.

At a lengthscale longer than that of the carbon rings, a nanoscale friction law (1) can be developed as follows. The average shear stress, $\langle\tau_{rz}\rangle$, for planar sliding interactions can be defined as $\langle\tau_{rz}\rangle \approx \langle f\rangle_{pull}/(A_{ss})$, where $\langle f\rangle_{pull}$ is the average force applied to the NT and A_{ss} is the common interfacial area during steady sliding. The strain rate, $\dot{\gamma}$, can be estimated by $\dot{\gamma} \approx \partial\langle V_z\rangle/\partial r$, where $\langle V_z\rangle$ is the average NT velocity in the z-direction and r is the radial distance. Then, the nanoscale analog of Newton's law for steady NT/polymer interfacial sliding is

$$\langle\tau_{rz}\rangle = \mu_{eff}\frac{\partial\langle V_z\rangle}{\partial r}, \tag{2}$$

where μ_{eff} is an effective viscosity for the NT/polymer interfacial sliding. As a result, an interfacial friction model for the entire NT pull-out process can be developed for the total shear stress, $\langle\tau_{rz}\rangle_{pull}$, which, in addition to the sliding component $\langle\tau_{rz}\rangle$, includes an initial threshold pull-out stress, τ_0:

$$\langle\tau_{rz}\rangle_{pull} = \tau_0 + \mu_{eff}\frac{\partial\langle V_z\rangle}{\partial r}. \tag{3a}$$

After approximating the change in velocity across the interfacial separation, $\bar{h}_{\text{VdW}}$, as the average NT velocity, $\langle V_z \rangle$, Eq. (3a) can be rewritten as

$$\langle \tau_{rz} \rangle_{\text{pull}} = \tau_0 + \mu_{\text{eff}} \frac{\langle V_z \rangle}{\bar{h}_{\text{VdW}}}, \qquad (3b)$$

where the strain rate is $\partial \langle V_z \rangle / \partial r \approx \langle V_z \rangle / \bar{h}_{\text{VdW}}$.

To complete the description of the interface model, the effective viscosity, μ_{eff}, should be described. The NT velocity is, on average, linearly related to the average applied force, $\langle f \rangle$ (Fig. 4), and the slope, χ_{eff}, can be determined. The resulting force–velocity dependence

$$\langle f \rangle = \chi_{\text{eff}} \langle V_z \rangle \qquad (4)$$

is an analog of the friction law in Eq. (2). The applied force, $\langle f \rangle$, in Eq. (4) is related to the shear stress in Eq. (2) by the force balance:

$$\langle f \rangle = \langle \tau_{rz} \rangle A_{\text{ss}}. \qquad (5)$$

Therefore, the viscosity coefficient, χ_{eff}, can be related to the effective viscosity μ_{eff} via

$$\mu_{\text{eff}} = \frac{\chi_{\text{eff}} \bar{h}_{\text{VdW}} / L_{\text{NT}}}{2\pi (R_{\text{NT}} + \bar{h}_{\text{VdW}}/2)}. \qquad (6)$$

Then, the interfacial friction model for the entire pull-out process is

$$\langle f \rangle_{\text{pull}} = f_0 + \chi_{\text{eff}} \langle V_z \rangle, \qquad (7)$$

where f_0 is the critical force.

5. Characterization of interfacial sliding

The interfacial friction model (7) involves the critical force, f_0, and the viscosity coefficient, χ_{eff}, which can be derived from MD simulation. For every incremental force loading, the NT velocity variations are plotted in Fig. 4 as a range represented by a vertical line. These ranges correspond to NT sliding velocity once the critical pull-out force, f_0, at 0.1 nN is reached. Then, the force–velocity dependence can be approximated by a linear relation (the solid line) [9], with a coefficient of $\chi_{\text{eff}} = 1.5 \pm 0.3$ (nN ps)/Å. This slope can be estimated from dashed lines like those shown in Fig. 4, which bound the NT velocity variations.

Once the value of the coefficient χ_{eff} is determined, the effective viscosity, μ_{eff}, can be calculated from Eq. (6) as 0.2 cP (centi-Poise) assuming an average separation, $\bar{h}_{\text{VdW}}$, of 3.4 A, the NT length, L_{NT}, of 53.65 A and the NT radius, R_{NT}, of 6.8 A. This result is close to the viscosity of pentane at 0.22 cP at room temperature [18].

Experimental characterization of the effective viscosity, μ_{eff}, can be performed by several methods. A direct method would be a NT pull-out test for a NT embedded in a polymer matrix [6]. Another method can be based on a quartz-crystal microbalance study [11] of the force required to slide atomic layers of carbon along a polymer surface. The scanning mode of atomic force microscopes can be also used for characterization of sliding friction [8,12]. So far, experimental evidence confirms the importance of the threshold force, a linear trend in the force–velocity relation [9] and the periodic effect of the atomic lattice on the sliding process [13].

6. Concluding remarks

Carbon nanotube (NT) pull-out from a crystalline polymer matrix is simulated via molecular dynamics (MD) and described by an interfacial friction model. Once steady sliding of the NT begins, a carbon-ring-based period in NT sliding velocity is observed. On average, interfacial interactions during NT sliding are approximated by a linear force–velocity relationship whose slope yields the effective viscosity coefficient in the friction model. A nanoscale friction law has been developed, which involves the pull-out force, an effective viscosity, and the strain rate, that are parameterized directly from the MD simulation.

written by W. Smith and T.R. Forester (Daresbury Laboratory, Warrington, UK, 1996).

References

[1] L.S. Schadler, S.C. Giannaris, P.M. Ajayan, Appl. Phys. Lett. 73 (1998) 3842.

[2] P.M. Ajayan, L.S. Schadler, S.C. Giannaris, A. Rubio, Adv. Mater. 12 (2000) 750.

[3] M.S.P. Shaffer, A.H. Windle, Adv. Mater. 11 (1999) 937.

[4] M.R. Piggott, Compos. Sci. Technol. 55 (1995) 269.

[5] V.T. Bechel, N.R. Sottos, Compos. Sci. Technol. 58 (1998) 1727.

[6] M.-F. Yu, B.S. Files, S. Arepalli, R.S. Ruoff, Phys. Rev. Lett. 84 (2000) 5552.

[7] S.J.V. Frankland, A. Caglar, D.W. Brenner, M. Griebel, J. Phys. Chem. B 106 (2002) 3046.

[8] B.N.J. Persson, Sliding Friction: Physical Principles and Applications, Springer, Berlin, 1998.

[9] B.N.J. Persson, Surf. Sci. Reports 33 (1999) 83.

[10] J. Krim, A. Widom, Phys. Rev. B 38 (1988) 12184.

[11] C. Daly, J. Krim, Phys. Rev. Lett. 76 (1996) 803.

[12] S. Okita, M. Ishikawa, K. Miura, Surf. Sci. 442 (1999) L959.

[13] S. Morita, S. Fujisawa, Y. Sugawara, Surf. Sci. Reports 23 (1996) 1.

[14] D.W. Brenner, O.A. Shenderova, J.A. Harrison, S.J. Stuart, B. Ni, S.B. Sinnott, J. Phys. C: Condens. Matter 14 (2002) 783.

[15] V.M. Harik, R.A. Cairncross, Mech. Mater. 32 (2000) 807.

[16] G.K. Batchelor, Introduction to Fluid Dynamics, Cambridge University Press, Cambridge, 1980.

[17] V.M. Harik, Solid State Commun. 120 (2001) 331.

[18] D.R. Lide (Ed.), CRC Handbook of Chemistry and Physics, 75th ed., CRC Press Inc., Boca Raton, 1994, pp. 6–243.